



---

---

## Soft Chemistry - Synthesis of Nano-Titanium-Doped-Tellurium-Cadmium for Solar Cell Applications

**Khaled M. Elsabawy**

Materials Unit, Chemistry Department, Faculty of Science, Tanta University, 31725 - Tanta, Egypt

Department of Chemistry, Faculty of Science, Taif University, 888 - Taif, Kingdom Saudi Arabia

E-mail address: [khaledelsabawy@yahoo.com](mailto:khaledelsabawy@yahoo.com) , [ksabawy@yahoo.com](mailto:ksabawy@yahoo.com)

### ABSTRACT

Soft chemistry procedures through sol-gel technique has applied to synthesize nano- Ti-doped CdTe composite. Gels were synthesized by the hydrolysis of a complex solution of  $\text{Si}(\text{OC}_2\text{H}_5)_4$ ,  $\text{Cd}(\text{CH}_3\text{COO})_2 \cdot 2\text{H}_2\text{O}$ ,  $\text{Ti}(\text{CH}_3\text{COO})_4$  and Te were heated from 350 to 600 °C in a  $\text{H}_2$ - $\text{N}_2$  atmosphere to form fine cubic CdTe doped crystals. The size of CdTe crystals, determined from the line broadening of X-ray diffraction pattern, increases from 6 to 21 nm in diameter with increasing heat-treatment temperature. Micro-structural features of Ti-doped CdTe crystals were characterized by both of AFM and SEM investigations . The analysis of micro-structural micrographs of both of SEM and AFM indicated that titanium additions improved the crystal growth of grain towards more lower grain size which ranged in between 1.4-2.5  $\mu\text{m}$  while 0.67  $\mu\text{m}$  through Scherrer's calculations.

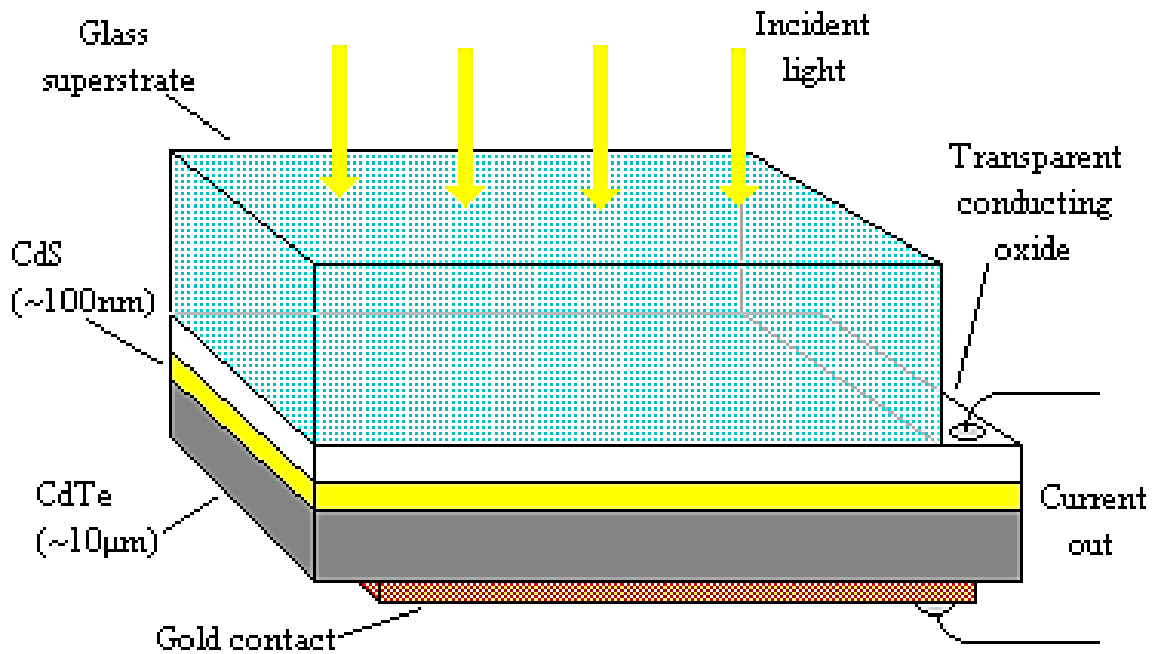
**Keywords:** Sol-Gel; Hydrolysis; AFM ; XRD; Microstructure; SEM

### 1. INTRODUCTION

Cadmium telluride (CdTe) solar cells are the basis of a significant technology with major commercial impact on solar energy production. Large-area monolithic thin film modules demonstrate long-term stability, competitive performance, and the ability to attract production-scale capital investments. This chapter reviews the status of CdTe thin-film solar

cells, with emphasis on the properties that make CdTe a favorable material for terrestrial photovoltaic solar energy conversion, their historical development, methods for device fabrication, analysis of device operation, and the fabrication strategies and technical challenges associated with present and future development of thin-film CdTe cells and modules.

Calculations of the dependence of ideal solar cell conversion efficiency on band gap show that CdTe is an excellent match to our sun, a G2 spectral-class star with an effective black-body photosphere surface temperature of 5700 K, and a total luminosity of  $3.9 \times 10^{33}$  erg/s. CdTe is a group IIB-VIA compound semiconductor with a direct optical band gap that is nearly optimally matched to the solar spectrum for photovoltaic energy conversion. The direct band gap,  $E_g = 1.5$  eV, and high absorption coefficient,  $>5 \times 10^5/\text{cm}$ , of CdTe means that high quantum yield can be expected over a wide wavelength range, from the ultraviolet to the CdTe band gap,  $\lambda = 825$  nm. Short-wavelength photons, with energy greater than  $E_g$ , are absorbed near the CdTe surface, making CdTe an attractive absorber-layer material for thin-film solar cells. The theoretical solar cell efficiency versus band gap for CdTe and the optical absorption coefficient versus energy for CdTe and other selected photovoltaic materials are compared in Figure 1 [1,2].



**Schematic Diagram of CdTe - component of solar cell.**

The high CdTe absorption coefficient,  $>5 \times 10^5/\text{cm}$ , for photons with  $E > E_g$  translates into 99% absorption of the absorbable AM1.5 photons within 2 µm of film thickness. CdTe emerged as a new electronic material in 1947 when Frerichs synthesized CdTe crystals by the reaction of Cd and Te vapors in a hydrogen atmosphere and measured their photoconductivity [3].

The early foundation for understanding the electronic nature of CdTe emerged from subsequent studies of single crystals purified by zone refinement. In 1954, Jenny and Bube [4] first reported that *p*-type and *n*-type conductivity could be obtained in CdTe by doping with foreign impurities. Shortly thereafter, Kandless and Site [5-8] showed that the conductivity type could also be changed by varying the Cd–Te stoichiometry. Cd excess yields *n*-type and Te excess yields *p*-type conductivity, as had been discovered for PbS, PbSe, and PbTe. In 1959, the *p*–*T*–*x* diagram of the Cd–Te system and its relationship to intrinsic conduction and extrinsic conductivity via foreign atom incorporation was established by Ebe [6], who proposed the existence of two electronic levels associated with Cd vacancies and one with interstitial Cd to account for the measured changes in conductivity at different temperature and Cd partial pressure. Furthermore, the electronic levels associated with In as an *n*-type dopant and Au as a *p*-type dopant were estimated. Loferski at RCA first proposed using CdTe for photovoltaic solar energy conversion in 1956 [1]. Although methods for controlling *n* and *p*-type conductivity in CdTe crystals were established by 1960, limited research was directed at the development of *p/n* homojunctions.

In contrast to *p/n* homojunction development, CdTe heterojunction solar cells have been widely investigated [9-14], proceeding along two paths, according to CdTe conductivity type. For *n*-type CdTe single crystals and polycrystalline films, extensive work was carried out on heterojunctions with *p*-type Cu<sub>2</sub>Te, *n*-type CdTe/*p*-type Cu<sub>2</sub>Te devices having a structure analogous to the CdS/Cu<sub>2</sub>S solar cell [15] were fabricated, by surface reaction of *n*-type single crystals or polycrystalline films in acidic aqueous solutions containing Cu salts for topotaxial conversion of CdTe to *p*-type Cu<sub>2</sub>Te [16–19]. The best thin-film CdTe/Cu<sub>2</sub>Te cells achieved cell efficiencies >7%, with VOC = 550 mV, JSC = 16 mA/cm<sup>2</sup> (60 mW/cm<sup>2</sup> irradiance), and FF = 50%, as reported by Kokate et al. [16].

Interestingly, these cells utilized an underlying 5-μm-thick *n*-type CdS layer to improve adhesion and electrical contact of the 20-μm-thick CdTe film on molybdenum substrates. Difficulty in controlling the Cu<sub>2</sub>Te formation process, poor device stability in CdTe/Cu<sub>2</sub>Te cells, and lack of a transparent *p*-type conductor ultimately shifted research emphasis to heterojunction structures employing *p*-type CdTe. Other work with *n*-type CdTe utilized Schottky barrier devices, formed by heating Pt or Au grids in contact with *n*-type CdTe single crystals [17] or electrodeposited CdTe thin films, with efficiencies approaching 9% [18].

For solar cells with single-crystal *p*-type CdTe, heterojunctions using stable oxides, such as In<sub>2</sub>O<sub>3</sub>:Sn (ITO), ZnO, SnO<sub>2</sub>, and CdS have been more widely investigated. In these devices, the short wavelength spectral response is influenced primarily by the transmission of the heteropartner and low-resistance contact, collectively referred to as the window layer.

Solar cells based on *p*-type CdTe single crystals with electron-beam evaporated indium–tin oxide (ITO) window layers with efficiencies = 10.5% were developed by the Stanford group, 1977, with VOC = 810 mV, JSC = 20 mA/cm<sup>2</sup>, and FF = 65% [20-22]. In 1987, cells made by the reactive deposition of indium oxide, In<sub>2</sub>O<sub>3</sub>, on *p*-type CdTe single crystals yielded total area efficiencies = 13.4%, with VOC = 892 mV, JSC = 20.1 mA/cm<sup>2</sup>, and FF = 74.5% [19]. In this device, the CdTe crystal had a carrier concentration of 6 × 10<sup>15</sup>/cm<sup>3</sup> and the CdTe (111) face was etched in bromine methanol prior to loading into vacuum for In<sub>2</sub>O<sub>3</sub> deposition. The VOC of this cell remains the highest ever reported for a CdTe device. Solar cells with ZnO window layers on *p*-type CdTe single crystals yielded poorer junction behavior, with efficiency <9% and VOC = 540 mV [20]. Cells made by evaporating *n*-type CdS films onto single-crystal *p*-type CdTe were first prepared by Tauc *et al.* and Sharma

[23,24], yielding conversion efficiencies less than 5%. Many researchers have reported The highest efficiency for a cell fabricated with thin-film CdS on *p*-type CdTe single crystal [25-29]. Their cell utilized 0.5- $\mu\text{m}$ -thick CdS deposited by chemical vapor deposition onto the (111) face of phosphorous.

The essential goal of the present investigations is achieving the possibility of synthesizing highly pure Ti-doped CdTe film with simple solution route to be applicable for solar cell aiming to promote its electrical features through low range of titanium doping.

## **2. EXPERIMENTAL**

### **2. 1. Doped Ti-Cd/Te Synthesis**

Pure CdTe layers and Ti-Doped CdTe were deposited on commercial glass substrates of 1 mm thickness by the CBD technique. 0.1M of Cadmium acetate and 0.05 M Titanium acetate solutions were prepared and 0.2 M of ammonia ( $\text{NH}_3$ ) was added drop wise until clear solution is obtained. Then 0.02 M of  $\text{TeO}_2$  is dispersed in 50 ml aqueous solution of  $\text{H}_2\text{SO}_4$ . Both solutions were magnetically stirred for 2 hrs under nitrogen atmosphere. Then two glass substrates were immersed into the solution for bath temperature 85 °C. After annealing treatment at 350 °C, 400 °C and 450 °C, the structural and SEM studies were made and analyzed. The reaction is:



### **2. 2. Structural and Microstructure measurements**

The X-ray diffraction (XRD) measurements were carried out at room temperature on the fine ground samples using  $\text{Cu-K}\alpha$  radiation source, Ni-filter and a computerized STOE diffractometer / Germany with two theta step scan technique.

Scannig electron microscopy (SEM): measurements were carried out along ab-plane using a small pieces of the prepared samples by using a computerized SEM camera with elemental analyzer unit Shimadzu (Japan). Atomic force microscopy (AFM): High-resolution Atomic Force microscopy (AFM) is used for testing morphological features and topological map (Veeco-di Innova Model-2009-AFM-USA). The applied mode was tapping non-contacting mode. For accurate mapping of the surface topology AFM-raw data were forwarded to the Origin-Lab version 6-USA program to visualize more accurate three dimension surface of the sample under investigation. This process is new trend to get high resolution 3D-mapped surface for very small area. The effect of annealing temperature on structural, and surface morphology properties has also been studied.

## **3. RESULTS AND DISCUSSION**

### **3. 1. Structural Features characterization**

The XRD pattern of the CdTe thin films prepared on glass substrates with bath composition 0.2 M cadmium acetate and 0.02 M tellurium dioxide at bath temperature 85 °C annealed at temperatures of 350 °C, 400 °C and 450 °C are shown in Figs. 1a-d. “The XRD pattern reveals that the deposited films are polycrystalline in nature as reported earlier [16]”.

The (111) peak corresponds to phase of polycrystalline structure of CdTe which lies at two theta ~ 38.3 degree as clear in Fig.1a. The strong and sharp diffraction peaks indicate the formation of well crystallized sample. It can be seen that the major peak (111) is strongly dominating the other peaks.

In Figs. 1b-d, the Ti-doped sample annealed at different temperatures 350 °C, 400 °C and 450 °C respectively also develop the weaker peaks (220), (311), and (331) for CdTe but weak the peak(111) as clear in Fig1b-d. The different peaks in the diffractogram were indexed and the corresponding values of inter planar spacing 'd' were calculated and compared with standard values of ICSD data (file no. 75-2086).

The height of (111) peak in X-ray diffraction patterns for CdTe thin films deposited at higher annealing temperature (450 °C) exhibit sharper peaks and small FWHM data see Fig. 1a.

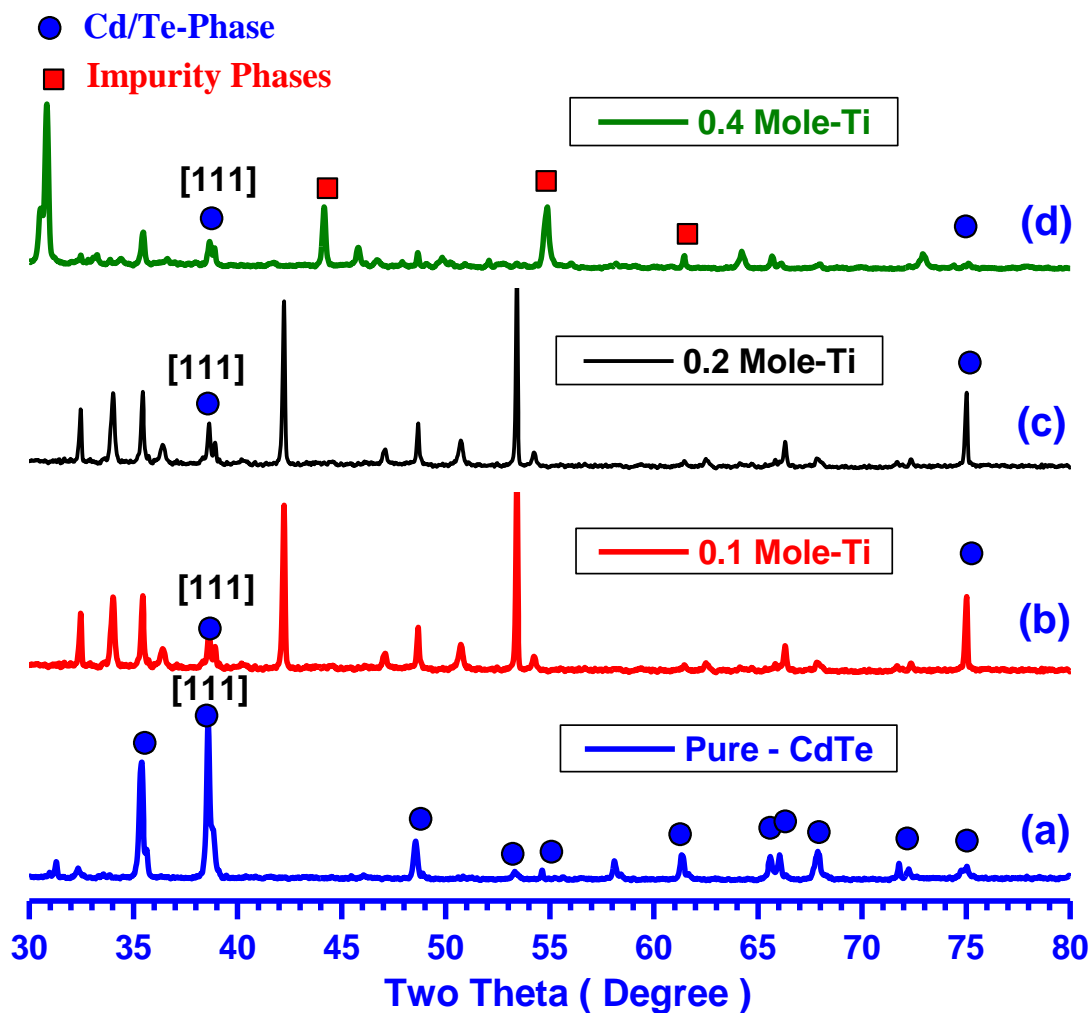


Fig. 1(a-d). X-ray diffraction patterns recorded for pure and variant Ti-doped CdTe.

As it clear from Fig. 1a-d the finger print of Cd/Te phase is highly detected in highly pure phase as clear in Fig. 1a but the characteristics peaks of CdTe-phase is shifted to lower intensity as Ti-additives increase as shown in Fig. 1b-d which reflects that titanium additions can be incorporated in the crystalline structure at low concentration of titanium doping (x = 0.1 mole) while at higher concentration Ti-ions are out of crystalline structure see Fig. 1d.

### 3. 2. Microstructural Features (SEM-measurements)

Fig. (2a-b) show the SEM-micrographs for pure and Ti-doped Cd/Te with x = 0.1 mole applied on the ground powders that prepared by solution route (SR). The average particle size was calculated and found to be in between 1.4 and 2.5 μm.

Samples were measured twice for more accurate and precise calculation of particle and grain sizes with two different magnification factors 5 and 10 μm respectively.

The EDX examinations for random spots in the same sample confirmed and are consistent with our XRD analysis for polycrystalline doped -CdTe composites, such that the differences in the molar ratios EDX estimated for the same sample is emphasized and an evidence for the existence of CdTe in highly pure phase with good approximate to the actual synthesised molar ratios (i.e. experimental molar ratios ~ theoretical molar ratios) which reflect quality of preparation of CdTe.

From Fig. 2a-b it is so difficult to observe inhomogeneity within the micrograph due to that the powders used are very fine and the particle size estimated is too small.

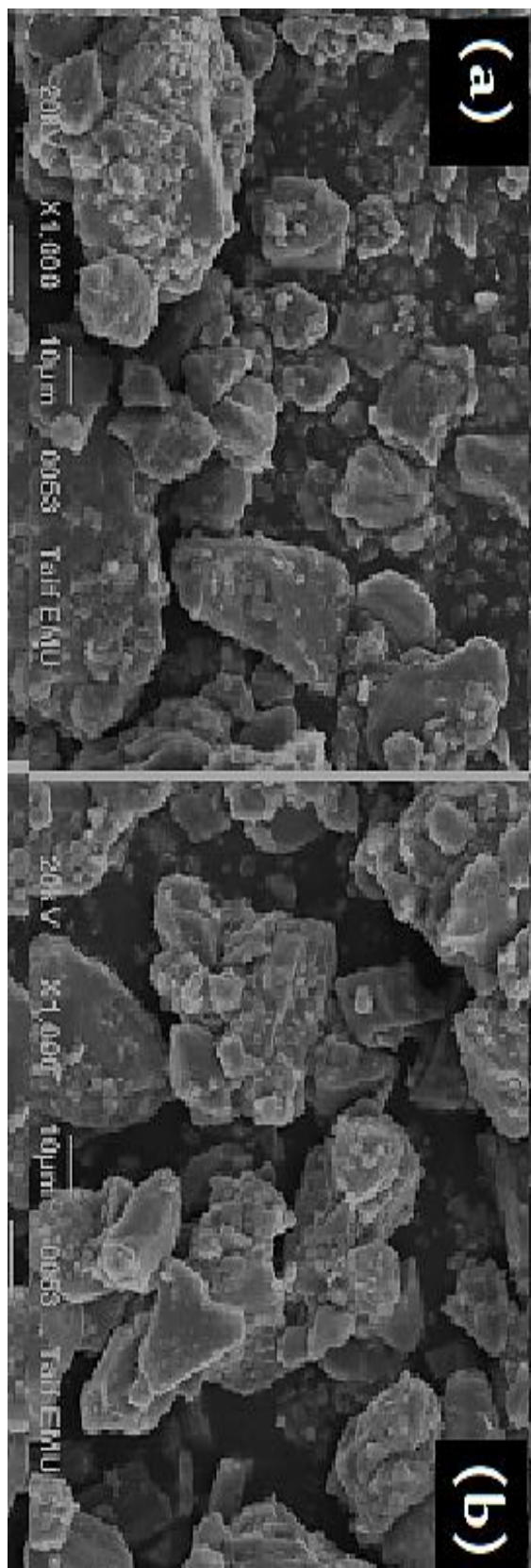
The grain size for CdTe-phase was calculated according to; Scherrer's formula [18],

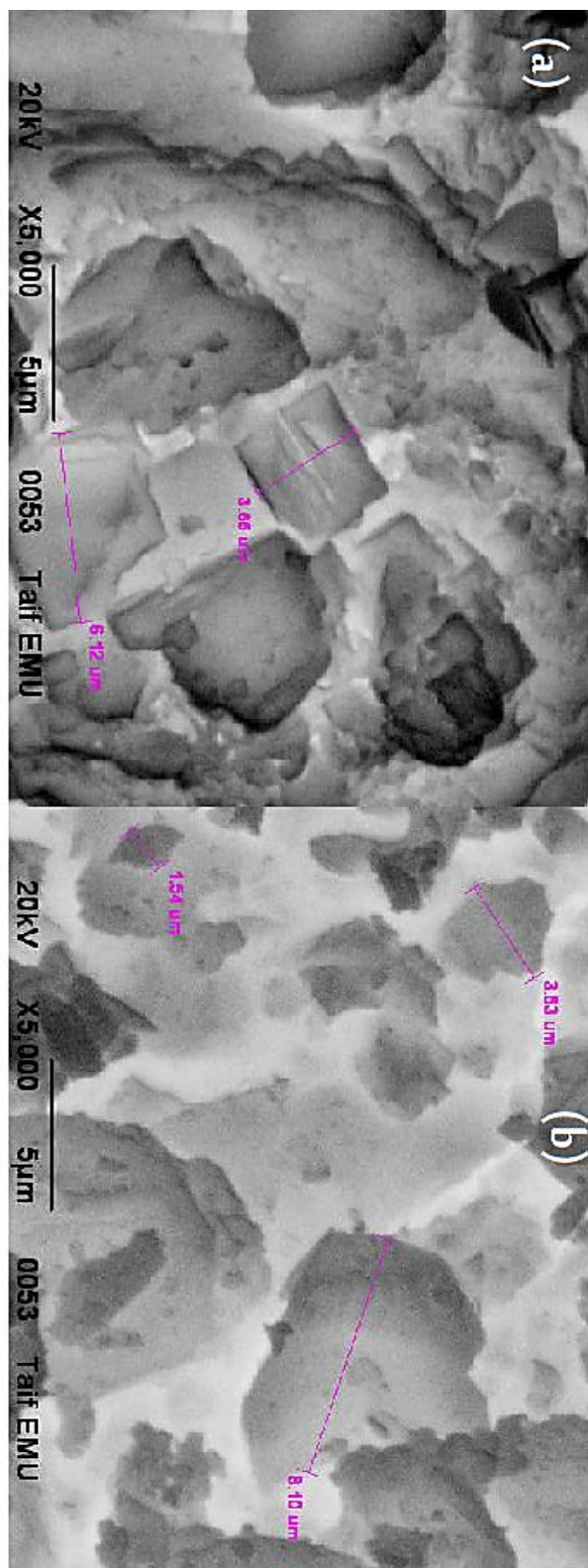
$$B = 0.87 \lambda/D \cos \theta \dots\dots\dots(1)$$

where D is the crystalline grain size in nm, θ, half of the diffraction angle in degree, λ is the wavelength of X-ray source ( Cu-K<sub>α</sub> ) in nm, and B, degree of widening of diffraction peak which is equal to the difference of full width at half maximum (FWHM) of the peak at the same diffraction angle between the measured sample and standard one.

From SEM-mapping, the estimated average grain size was found to be (1.4 -2.5 μm) which is relatively large in comparison with that calculated applying Scherrer's formula for Ti-doped-CdTe (D ~ 0.67 μm).

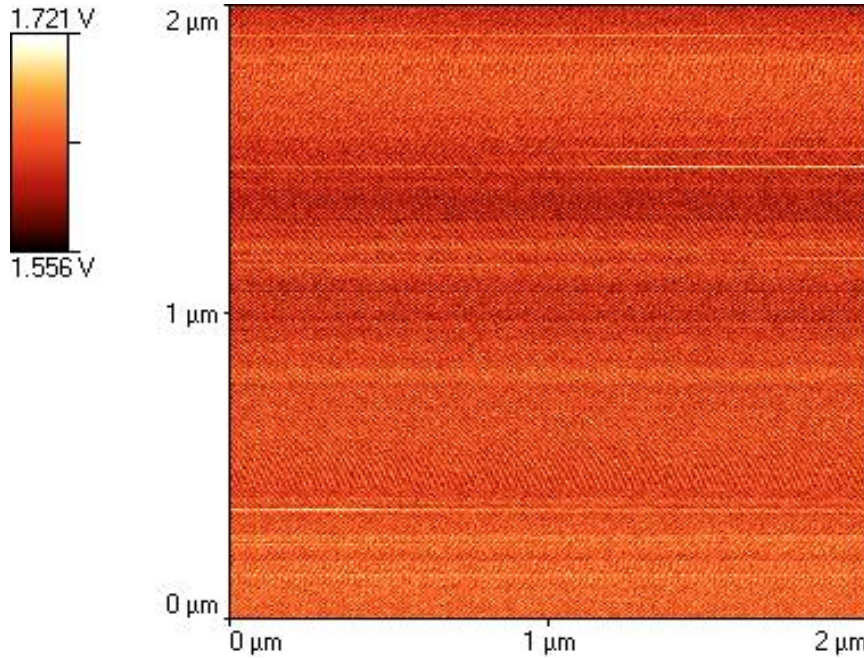
This indicates that, the actual grain size in the material bulk is smaller than that detected on the surface morphology. Furthermore, in our EDX (energy disperse X-ray) analysis, Ti<sup>4+</sup> was detected qualitatively with good approximate to the actual molar ratio but not observed at Cd/Te grain boundaries which confirm that Ti-ions has diffused regularly into material bulk of CdTe-phase and Ti<sup>4+</sup>-ion induces in the crystalline structure through solid state reaction by some extent only at low doping concentration x = 0.1 mole see Fig. 1a.





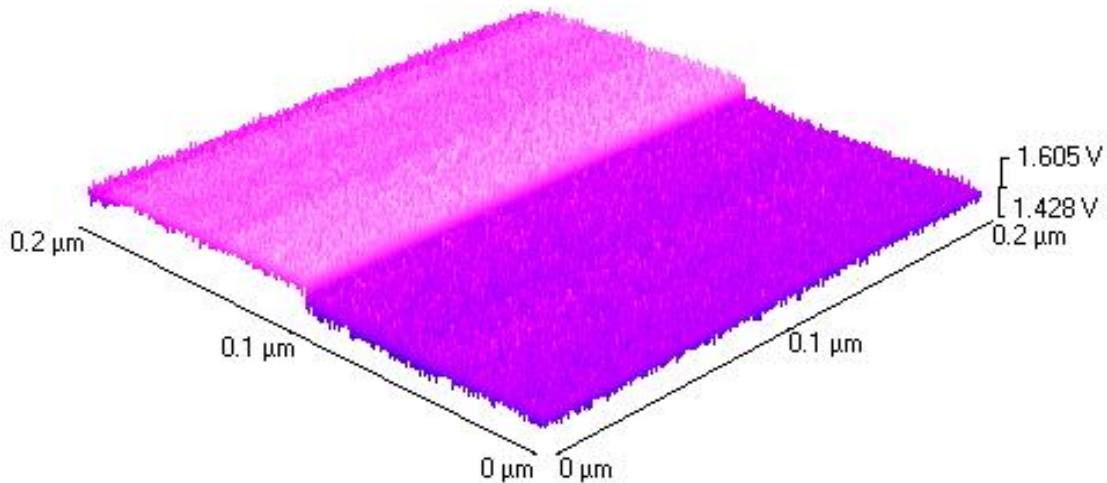
**Fig. 2(a-b).** SE-micrographs recorded for pure Cd/Te and Ti-added- CdTe (x = 0.1 mole) with to magnification factor 5 and 10 μm respectively.

### 3. 3. Atomic Force Microscopy Investigations



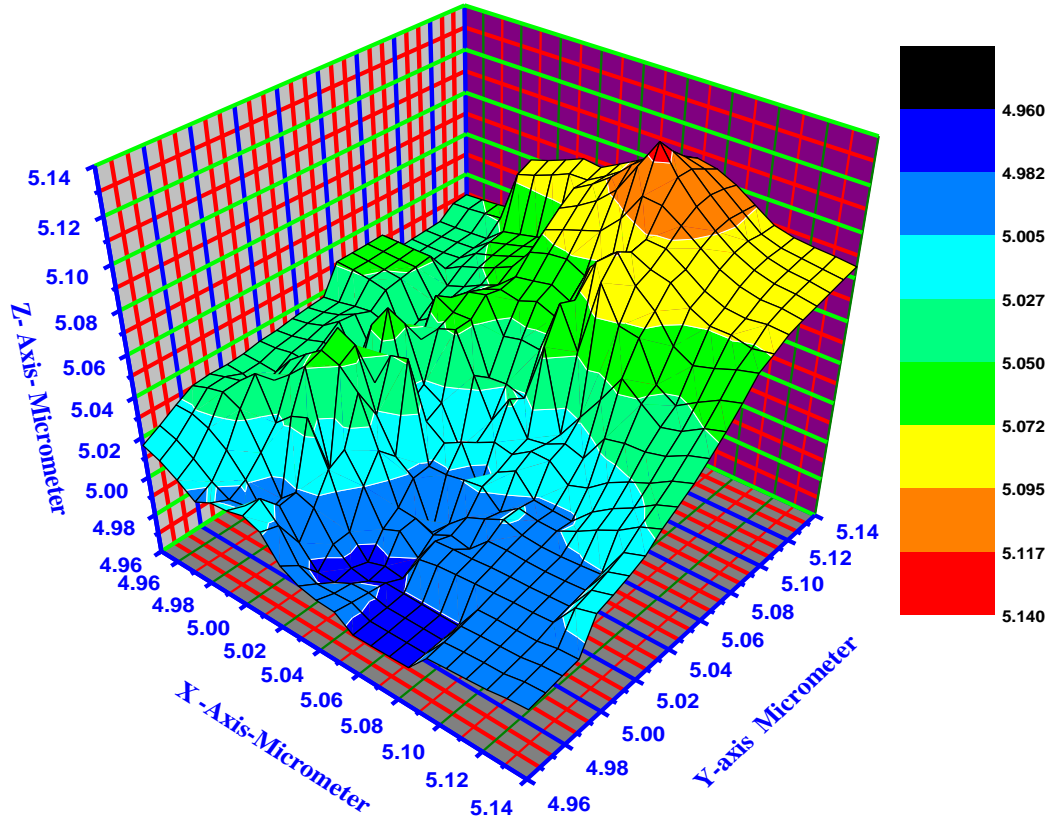
**Fig. 3(a).** 2D-AFM-micrograph tapping mode image recorded for scanned area  $2 \times 2 \mu\text{m}^2$  of CdTe Thin film.

Fig. 3a shows 2D-AFM-micrograph tapping mode image recorded for scanned area  $2 \times 2 \mu\text{m}^2$  of Ti-doped CdTe Thin film . The analysis of inter-layers structure of the surface using high resolution imaging of tapping AFM indicated that the distances between layers of CdTe film are nearly equals within the range  $0.2\text{-}0.25 \mu\text{m}$  which confirms why Ti-doped CdTe used as equi-potential surfaces in the advanced solar cell structure.



**Fig. 3(b).** 3D-AFM-micrograph tapping mode image recorded for scanned area  $0.2 \mu\text{m}^2$  of Ti-doped CdTe Thin film.

Fig.3b displays 3D-AFM-micrograph tapping mode image recorded for scanned area  $0.2 \mu\text{m}^2$  of Ti-doped CdTe Thin film .The analysis of this micrograph indicated that there are two different axial levels through z-axis as clear in the micrograph the first level colored by deep violet ( lower level ) and the other higher level is colored with pink color. This differentiations in the surface level could be useful in the application Ti-doped CdTe junction of electronics devices specially if it is used as heterogeneous doped junction .



**Fig. (3c).** 3D-visualized-contour plot of AFM-micrograph surface image recorded for scanned area  $0.2 \mu\text{m}^2$  of Ti-doped CdTe-film.

Fig. 3c shows 3D-visualized-contour plot of AFM-micrograph surface image recorded for scanned area  $0.2 \mu\text{m}^2$  of Ti-doped CdTe-film .For accurate mapping of the surface topology AFM-raw data were forwarded to the Origin-Lab version 9-USA program to visualize more accurate three dimension surface of the sample under investigation.

The analysis of this figure can be summarized the following topographic facts;

- Total scanned area  $0.04 \mu\text{m}^2$ .
- There are five gradient of heights surface the 1<sup>st</sup> one is red zone which represents ~ 2% of the scanned area with height higher than  $6.14 \mu\text{m}$ , the 2<sup>nd</sup> zone which represents ~9% is colored by orange with heights gradient  $6.11-6.08 \mu\text{m}$ , the 3<sup>rd</sup> zone represented by yellow color occupies ~14% of the whole scanned area with gradient  $5.072-5.095$

$\mu\text{m}$ , the 4<sup>th</sup> zone which represents major heights gradient with green color ~39% and the 5<sup>th</sup> zone is the lowest heights gradient by pale and dark blue coloration with heights gradient ranged in between (4.96-5.005  $\mu\text{m}$ ).

#### 4. CONCLUSIONS

Simple and fast solution route synthesis was succeeded to synthesized highly pure film of Ti-doped CdTe film with very low doping ratio  $x = 0.1$  mole. The analysis of microstructural micrographs of both of SEM and AFM proved that titanium additions make as splitter and improved the crystal growth of grain towards more lower grain size which ranged in between 1.4-2.5  $\mu\text{m}$  while it estimated from XRD and found to be 0.67  $\mu\text{m}$  via Scherrer's calculations.

#### References

- [1] The Mora-Sero, R. Tena-Zacra, J. Gozalez, V. Munoz Sanjose, *J. Crys Growth* 262, 19 (2004).
- [2] C. S. Feretides, D. Marinskiy, V. Viswanathan, B. Tetall, V. Palekis, P. Selvaraj, D.L Morel, *Thin solid films*, 361-362, 520 (2000).
- [3] G.M. Li., R.A. Zingaro, M. Segi, J.H. Reibenspies, T. Nakajima, *Organometallics* 756 (1997).
- [4] G.M Li, R.A. Zingaro, *J. Chem. soc. perkin Trans. 1*, 647 (1998)
- [5] B.E. McCandless, J.R. Sites, in; Luque, A. Hegedus. S.(Eds), *Handbook of Photovoltaic Science and Engineering*, John Wiley & Sons, (617-662) 2003.
- [6] M. S. Han, T. W. Kang, J.H. Leem, M.H. Lee, K.J. Kim, T.W. Kim, *J. Appl. Phys.* 82, 6012 (1997).
- [7] S. Rujirawat, Y. Xin, N. D. Browning, S. Sivananthan, D. J. Smith, S. -C. Y. Tsen, Y. P. Chen, V. Nathan, *Appl. Phys. Lett.* 74, 2346 (1999).
- [8] H. Ebe, T. Okamoto, H. Nishino, T. Saito, Y. Nishijima, M. Uchikoshi, M. Nagashima, H. Wada, *J. Electron. Mater.* 25, 1358 (1996).
- [9] R. Chou, M. Lin, K. Chou, *Appl. Phys. Letts.* 48, 523 (1986).
- [10] I. Baht, W.S. Wang, *Appl. Phys. Letts.* 64, 566 (1994).
- [11] J. H. Pei, C.M. Lin, D. S. Chou, *Chin. J. Phys.* 36, 44 (1998).
- [12] H. Nishino, Y. Nishijima, *J. Cryst. Growth* 167, 488 (1996).
- [13] R. Korenstein, P. Madison, P. Hallock, *J. Vac. Sci. Technol. B* 10, 1370 (1992).
- [14] H. Tatsuoka, H. Kuwabara, Y. Nakanishi, H. Fujiyasu, *J. Cryst. Growth* 129, 686 (1993).

- [15] M. Stoel- Lerma, Ralph. A. Zingaro, S.J. Castillo, *Journal of Oregano Metallic Chemistry* 623, 81-86 (2001).
- [16] A.V. Kokate, M.R. Asabe, P.P. Hankare, B.K. Chougule, *Journal of Physics and Chemistry of Solids* 68, 53-58 (2007).
- [17] [A.V. Kokate, U.B. Suryavanshi, C.H. Bhosale, *J. Sol. Energy* 80, 156 (2006).
- [18] T.L. Chu, S.S. Chu, J. Britt, C. Ferekides, C. Wang, C.Q. Wu, H.S. Ullal, *Electron. Device Lett.* 13 (1992) 303.
- [19] J. Britt, C. Ferekides, *Appl. Phys. Lett.* 62 (1993) 2851.
- [20] T. Gruszecki, B. Holmstrom, *Solar Energy Materials and Solar Cells*, vol. 31, North Holland, 1993 (pp. 227 ±234).
- [21] N. Nakayama, et al., *Sol. Energy Mater. Sol. Cells* 35 (1994)271-278.
- [22] M.S. Shaalan, J. Muller, *Sol. Cells* 28 (1990) 185-193.
- [23] J. Tauc, in: J. Tauc (Ed.), *Amorphous and Liquid Semiconductors*, Plenum Press, New York, 1974 (p. 159).
- [24] T.P. Sharma, et al., *C.S.I.O. Commun.* 19(3-4) (1992) 63-66.
- [25] O.S. Heavens, *Optical Properties of Thin solid Films*, Dover, New York, 1965.
- [26] S.M. Sze, *Physics of Semiconductor Devices*, Wiley, New York, 1979.
- [27] S.K. Sharma, PhD Thesis, C.C.S. University, Meerut, India, 1998.
- [28] C. Crevecoueur, *Phys. Lett. A* 33 (1) (1970) 25.
- [29] D.B. Sharma, P. Kasyap, O.P. Agnihotri, *Physics of Semiconductor Devices*, in: V. Kumar, S.K. Agarwal (Eds.), Narosa-Publishing House, New Delhi, India, 1998.

( Received 02 January 2016; accepted 14 January 2016 )